Li7La3Zr2O12 (LLZO): An Overview

Subjects: Electrochemistry | Engineering, Electrical & Electronic

Contributor: Md Mozammal Raju

Li7La3Zr2O12 (LLZO) is an inorganic garnet type solid electrolyte which has proven to be one of the most promising electrolytes because of its high ionic conductivity at room temperature, low activation energy, good chemical and electrochemical stability, and wide potential window.

LLZO | solid-state electrolyte | first-principles computing | synthesis | doping | lithium ionic conductivity

1. Introduction

Among many energy storage devices, lithium-ion battery has been the most commonly used technology because of its advantages including high energy density, long duty cycle, low self-discharge, and light weight [1][2][3]. However, there are some concerns about lithium-ion batteries like: safety issues because of the formation of dendrites, reduced power capability because of the formation of solid electrolyte interface (SEI) from continuous charging and discharging, low ionic conductivity, and high cost compared to other existing rechargeable batteries. Extensive research is being carried out by many groups to resolve these issues aiming to improve the performance of lithium-ion batteries.

Electrolyte is one of the most important parts that determine the performance of lithium-ion batteries. According to the state of form, electrolyte materials can be categorized as liquid electrolytes, polymer electrolytes, ionic electrolytes, and solid electrolytes.

Research has been performed on various types of inorganic solid electrolyte: Li_3N type, [4][5][6] LISICON type, [7][8][9] NASICON type, [10][11][12][13][14][15][16][17] beta alumina type, [18][19][20][21][22] LIPON type, [23][24][25] and perovskite type; [26][27] but the problems with these types of inorganic electrolytes are: (1) poor chemical stability due to the reaction with metal electrodes, (2) difficulty to prepare, (3) a low electrochemical voltage window, and (4) low ionic conductivity.

In 2003, Thangadurai et al. first reported the use of inorganic garnet-type lithium oxide with a nominal composition of $Li_5La_{3\times2}O_{12}$ (X = Nb, Ta) for ASSB and showed the promising capability in overcoming the problems mentioned above [28]. In 2007, the same group reported the most promising garnet-type Li oxide with nominal composition of $Li_7La_3Zr_2O_{12}$, also known as LLZO, which revealed excellent properties with exceptional results that exceeded all the previous findings of solid electrolytes [29]. Since its first report, LLZO has drawn great attention of the battery

research community; in order to use in practical purpose application a considerable amount of research has been undertaken to increase the performance of LLZO.

In 2015, Ramakumar et al. reported that among all garnet-type electrolytes, LLZO with a composition of $Li_7La_3Zr_2O_{12}$ exhibits the highest ionic conductivity corresponding to the lowest activation energy [30]. At 33 °C, $Li_7La_3Zr_2O_{12}$ composition exhibited a total (bulk + grain boundary) ionic conductivity of 5×10^{-4} S/cm with an activation energy of 0.32 eV. However, with further increasing Li content, the total ionic conductivity starts to decrease; in the case of 7.5 molar unit of Li content, the conductivity drops to 1×10^{-4} S/cm with the activation energy increasing to 0.38 eV [30].

2. Structural Analysis of LLZO

In 2003, Thangadurai et al. reported $Li_5La_3M_2O_{12}$ (M = Nb, Ta) oxides as a fast garnet-like Li-ion conductor [28]. Later in 2007, from the same group Murugan et al. introduced a new garnet-type material $Li_7La_3Zr_2O_{12}$ known as LLZO which has higher ionic conductivity at room temperature [29]. The generic formula for LLZO garnet $Li_7La_3Zr_2O_{12}$ was derived from the garnet type family $Li_7A_3B_2O_{12}$, in which Li ions occupy octahedral and tetrahedral sites, A-cations belong to eight-coordination sites and B-cations belong to six-fold coordination sites. LLZO exhibits two phases, namely tetragonal phase (lattice parameter: a = b ≠ c, angle: α = β = γ = 90°, space group $I4_1/acd$) and cubic phase (lattice parameter: a = b = c, angle: α = β = γ = 90°, space group Ia3'd). Both phases possess the same structural framework but there is a difference in the distribution of Li atoms, which dominantly determines the ionic conductivity of LLZO. In the tetragonal phase, Li ions can occupy tetrahedral 8a, and octahedral 16f and 32g sites as shown in **Figure 1**, [31] where Li(1) is in 8a tetrahedral site connected to four O atoms; Li(2) and Li(3) belong to 16f and 32g octahedral sites, respectively, and both are connected to six O atoms. Unlike the tetragonal phase, Li in cubic structure occupies only 2 different sites namely 24d tetrahedral sites and 96h octahedral sites as shown in **Figure 2** [32]. Therefore, it is clear from the site occupancy perspective that in the cubic phase Li ions have more available sites for migration than in the tetragonal phase.

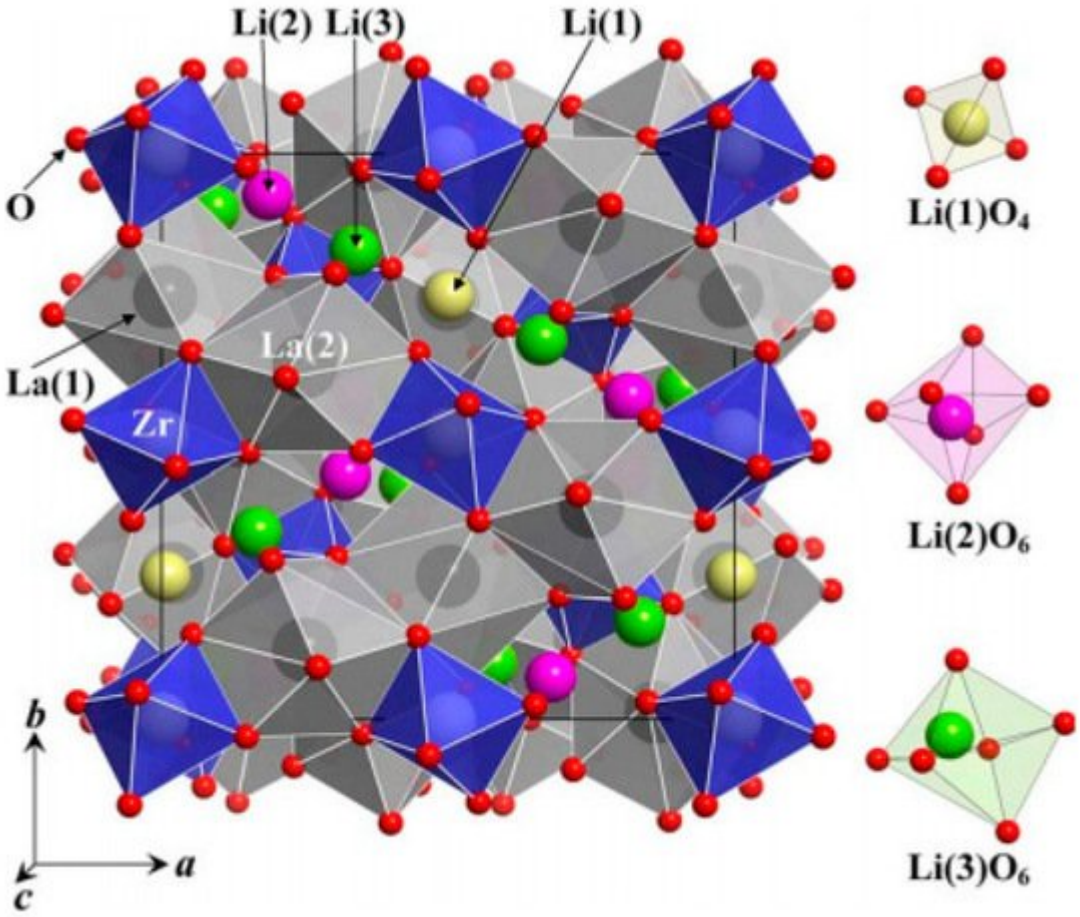

Figure 1. Crystal structure of a unit cell of 8 per formula unit (pfu) in tetragonal LLZO ($Li_7La_3Zr_2O_{12}$). Shown on right side are three different lithium sites: 8a, 16f and 32g (reprinted from [31]).

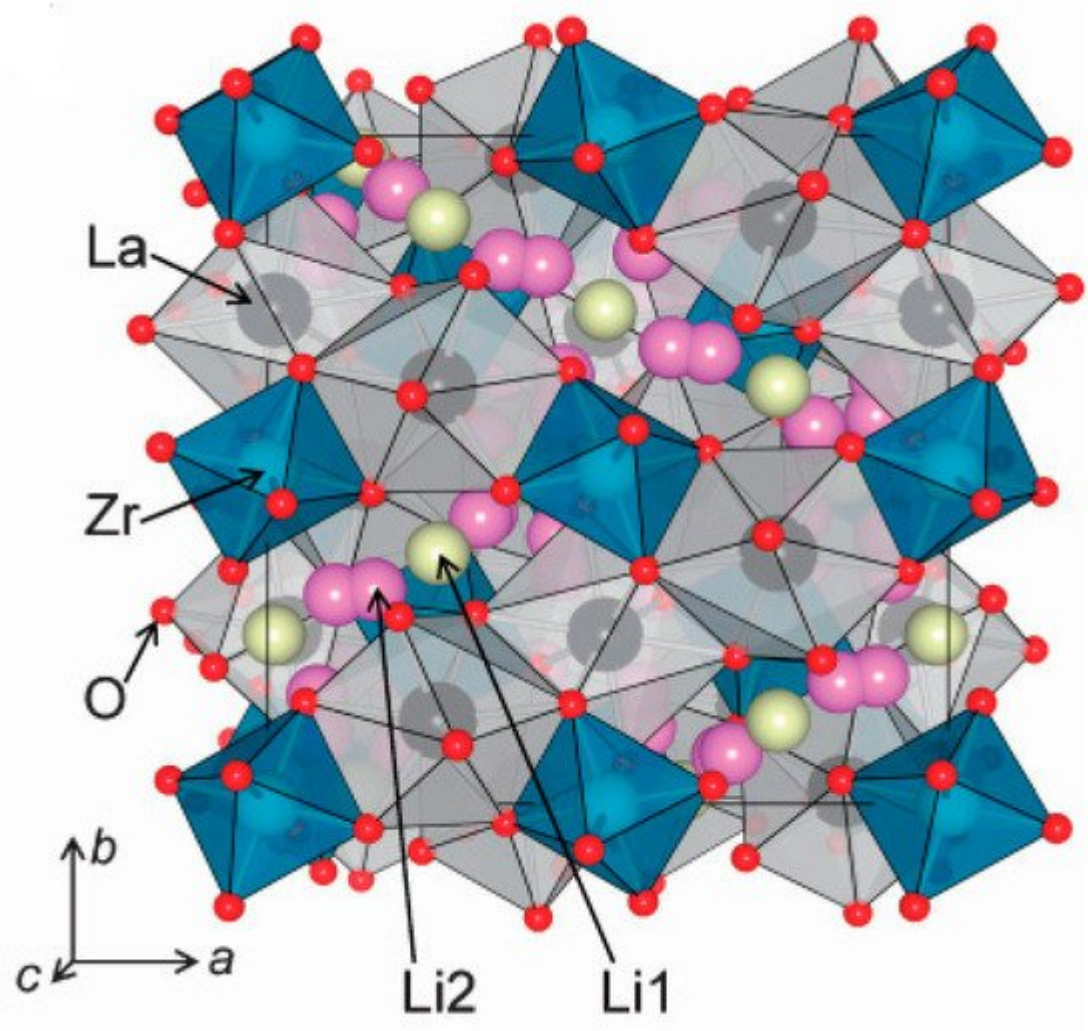

Figure 2. Crystal structure of a unit cell of 8 pfu cubic LLZO, where Li1 white spheres represent 24d tetrahedral sites and Li2 pink spheres represent 96h octahedral sites (reprinted from [32]).

Therefore, for an 8 per formula unit (pfu) LLZO cell which has 56 Li atoms, the total number of positions available for Li atoms in tetragonal phase is 56 (tetrahedral 8a, octahedral 16f and 32g), but in cubic phase the total number of positions available for Li atoms is 120 (tetrahedral 24d, octahedral 96h). In other words, in the cubic phase Li has 64 empty positions available for migration, but in the tetragonal phase all the positions (the sites 8a, 16f and 32g) are filled—and thus there is no vacancy for movement of Li as shown in **Figure 3**a [32]. According to Awaka et al., in cubic-phase LLZO the tetrahedral sites are more likely to be occupied than octahedral sites as shown in **Figure 3**b, where more vacant octahedral sites are available to be occupied [31]. Similar hypothesis has been given by Bernstein et al. [33] as shown in **Figure 4**, according to Bernstein the 8a sites which are filled in the tetragonal phase are identified as 24d in cubic phase are almost filled; while 16f and 32g sites which are full in the tetragonal phase are identified as 96h in the cubic phase which has more empty positions available (because of Coulomb repulsion) to be filled [33].

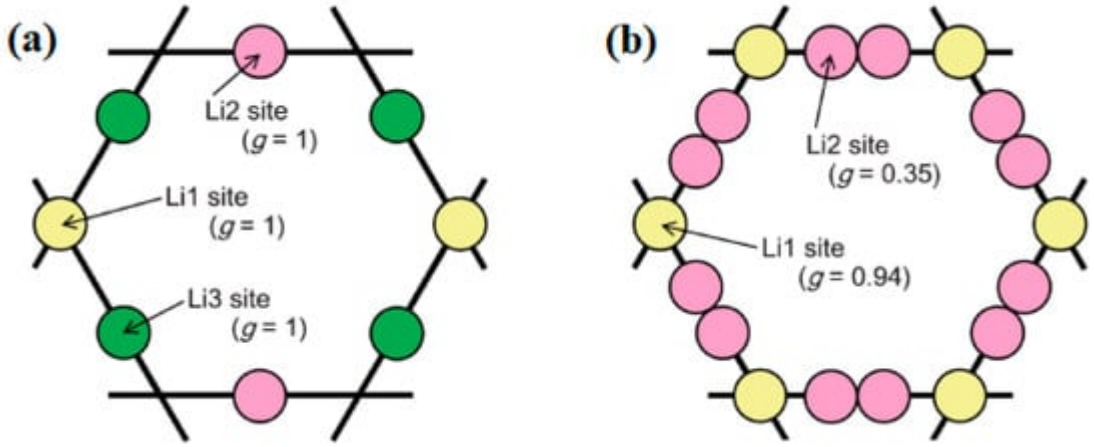

Figure 3. Loop structure of Li arrangement in (**a**) tetragonal phase where Li1, Li2 and Li3 represent 8a, 16f and 32g site, respectively, (**b**) cubic phase where Li1 and Li2 represent 24d and 96h site, respectively, and g denotes the occupancy for each site (reprinted from [32]).

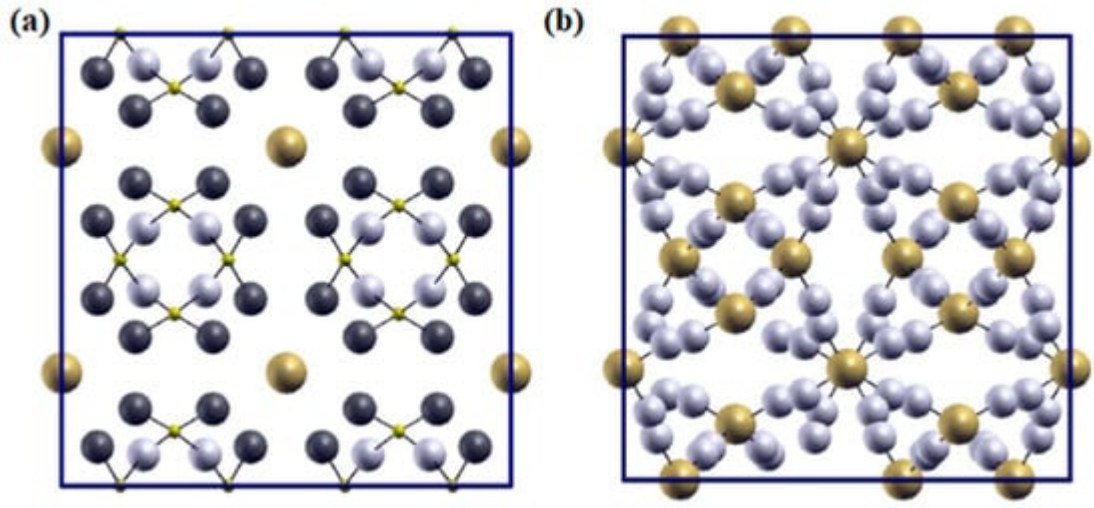

Figure 4. Two-dimensional view of (**a**) tetragonal phase where large gold, white and dark grey spheres represent 8a, 16f and 32g sites, respectively, and (**b**) cubic phase where all the possible 120 positions of Li are represented by gold and white spheres corresponding to 24d and 96h sites, respectively (reprinted from [33]).

Awaka and Bernstein suggested higher occupancy of tetrahedral sites than octahedral sites [32][33]; however, a simulated study done by Meier et al., using the first principles method with molecular metadynamics on CP2K, found the opposite scenario [34][35]. They took 120 randomly generated structures where 56 Li atom can fill 72 available sites (considering 48 octahedral sites because two neighboring octahedral sites cannot be occupied) obeying Coulomb repulsion; they found very interesting and convincing results which indicate that the cubic phase LLZO octahedral site has higher occupancy than the tetrahedral site. They have shown that the most stable structure is the structure that possesses the lowest potential energy, in which Li atoms occupy 11 out of 24 tetrahedral sites (about 46%) and 45 out of 48 octahedral sites (about 94%).

3. Synthesis Techniques of LLZO (Li7La3Zr2O12)

The first LLZO was prepared by Murugan et al. in 2007 using solid state reaction technique where they used sintering temperature of 1230 °C for 36 h [29]. After 2007 this became the most widely used method; however, some researchers reported some concerns regarding this process: (1) the method is difficult in achieving desired stoichiometric structure, (2) high sintering temperature introduces impure phases into the system, (3) the long period of high sintering processing causes too much Li loss from the system, and (4) at high temperature, other foreign elements are introduced from the crucible containing the sample [36][37].

To avoid the problems arising from high sintering temperatures during solid state reaction, which causes Li loss and creates impure phase formation in the system, the sol-gel method has been developed which involves hydrolysis and polymerization. The sol-gel method uses relatively low temperatures and yields uniformly distributed finer sized particles without needing intermittent grinding [38].

The Pechini method is a modified technique of the sol-gel method which involves the ability to chelate metal ions with the help of carboxylic acids such as tartaric acid, citric acid, etc. and forms a polymeric resin due to polysensitization when heated with polyethylene glycol or another hydroxylic alcohol agent. This process requires lower sintering temperature, shorter reaction time and yields uniformly distributed nanosized particles. Using the Pechini method, Gao et al. synthesized Li 5La 3Bi 2O 12 nanocrystalline powder [39], and Jin et al. synthesized stable cubic Al-doped LLZO [40].

Pulsed laser deposition (PLD) has also been used for the fabrication of LLZO. In PLD, a laser beam usually ablates the targets at a suitable angle which helps to preserve the stoichiometry and composition of the target. PLD is very flexible process as it allows the adjustment of conditions that are appropriate for deposition such as the energy of laser density, temperature, and pressure. Also, it reduces the Li loss that occurs during the synthesis process as it allows films to be grown at low temperature in a shorter period. However, a very few studies have been reported so far that used PLD for LLZO preparation. The effect of different substrates on the growth of LLZO at different deposition temperature were investigated by Park et al. [41]. Tan et al. used this method to prepare LLZO on sapphire and SrTiO 3 substrates [42].

4. Sintering Techniques of LLZO

Sintering is one of the most important steps during the fabrication of solid-state electrolytes as it plays a vital role in densifying the pellet of electrolyte. Dense pellets have many advantages such as: (1) decreasing grain boundary resistance and thus decreasing the activation energy to increase the Li ionic conductivity, (2) suppressing the formation of dendrites and accordingly increasing the safe operation of the battery, and (3) increasing the mechanical strength of the battery. Being not dense enough or possessing high porosity in the solid electrolyte increases the chance of fragility, and hence may cause mechanical failure of the device. There are some techniques like furnace sintering [29], hot pressing [37], field assisted sintering technology (FAST) [43] and spark plasma sintering (SPS) [44] reported in the literature that can be used to improve the density of pellets.

Hot pressing involves heat and pressure, where samples are sintered at high temperatures under a certain pressure. Simultaneous application of high temperature and pressure used in this process helps to stabilize the structure and densifies the pellets better. This method is also known as hot isostatic pressing (HIP).

Field-assisted sintering technology (FAST) is a sophisticated modern technology used to sinter samples at a high heating rate. The process of FAST is similar to that of hot isostatic pressing (HIP), however, a dc current passes through the tool along with the uniaxial pressure to assist in sintering process. In other words, the additional heat is generated by an external electrical circuit. FAST has many advantages over other sintering methods in terms of the fast-sintering process that saves time and reduction in Li ion loss that usually occurs due to a long sintering duration. As the synthesis of raw materials and sintering are done together at one time, it avoids the process of tedious intermittent grinding and repeated long-time sintering.

References

1. Etacheri, V.; Marom, R.; Elazari, R.; Salitra, G.; Aurbach, D. Challenges in the development of advanced Li-ion batteries: A review. Energy Environ. Sci. 2011, 4, 3243–3262.
2. Tarascon, J.-M.; Armand, M. Issues and challenges facing rechargeable lithium batteries. Mater. Sustain. Energy 2010, 171–179.
3. Scrosati, B.; Hassoun, J.; Sun, Y.-K. Lithium-ion batteries. A look into the future. Energy Environ. Sci. 2011, 4, 3287–3295.
4. Gregory, D.H.; O'Meara, P.M.; Gordon, A.G.; Hodges, J.P.; Short, S.; Jorgensen, J.D. Structure of Lithium Nitride and Transition-Metal-Doped Derivatives, Li3-x-yMxN (M = Ni, Cu): A Powder Neutron Diffraction Study. Chem. Mater. 2002, 14, 2063–2070.
5. Zintl, E.; Schneider, A. Röntgenanalyse der Lithium-Zink-Legierungen (15. Mitteilung über Metalle und Legierungen). Z. Elektrochem. Angew. Phys. Chem. 1935, 41, 764–767.
6. Alpen, U.V.; Rabenau, A.; Talat, G.H. Ionic conductivity in Li3N single crystals. Appl. Phys. Lett. 1977, 30, 621–623.
7. Kanno, R.; Murayama, M. Lithium Ionic Conductor Thio-LISICON: The Li2S-GeS2-P2S5 System. J. Electrochem. Soc. 2001, 148, A742–A746.
8. Abrahams, I.; Bruce, P.; West, A.; David, W. Structure determination of LISICON solid solutions by powder neutron diffraction. J. Solid State Chem. 1988, 75, 390–396.
9. Bruce, P.; West, A. Ionic conductivity of LISICON solid solutions, Li2+2xZn1−xGeO4. J. Solid State Chem. 1982, 44, 354–365.
10. Von Alpen, U.; Bell, M.F.; Höfer, H.H. Ionic conductivity in Na4ZrSi3O10. Solid State Ionics 1982, 7, 345–348.

11. Hong, H.-P. Crystal structures and crystal chemistry in the system Na1+xZr2SixP3−xO12. Mater. Res. Bull. 1976, 11, 173–182.
12. Golub, A.; Shumilova, I.; Zubavichus, Y.; Slovokhotov, Y.; Novikov, Y.; Marie, A.; Danot, M. From single-layer dispersions of molybdenum disulfide towards ternary metal sulfides: Incorporating copper and silver into a MoS2 matrix. Solid State Ionics 1999, 122, 137–144.
13. Aono, H.; Sugimoto, E.; Sadaoka, Y.; Imanaka, N.; Adachi, G. ChemInform Abstract: The Electrical Properties of Ceramic Electrolytes for LiMxTi2-x(PO4)3 + yLi2O, M: Ge, Sn, Hf, and Zr Systems. J. Electrochem. Soc. 1993, 140, 1827.
14. Ivanov-Schitz, A. Ionic conductivity of the NaZr2(PO4)3 single crystals. Solid State Ionics 1997, 100, 153–155.
15. Knauth, P. Inorganic solid Li ion conductors: An overview. Solid State Ionics 2009, 180, 911–916.
16. Alamo, J.; Roy, R. Crystal chemistry of the NaZr2(PO4)3, NZP or CTP, structure family. J. Mater. Sci. 1986, 21, 444–450.
17. Goodenough, J.B.; Hong, H.-P.; Kafalas, J. Fast Na+-ion transport in skeleton structures. Mater. Res. Bull. 1976, 11, 203–220.
18. Sudworth, J. The sodium/sulphur battery. J. Power Sources 1984, 11, 143–154.
19. Beevers, C.A.; Ross, M.A.S. The Crystal Structure of “Beta Alumina” Na2O·11Al2O3. Z. Krist. Cryst. Mater. 1937, 97, 59–66.
20. Farrington, G.; Dunn, B.; Briant, J. Li+ and divalent ion conductivity in beta and beta″ alumina. Solid State Ionics 1981, 3–4, 405–408.
21. Bettman, M.; Peters, C.R. Crystal structure of Na2O.MgO.5Al2O3 [sodium oxide-magnesia-alumina] with reference to Na2O.5Al2O3 and other isotypal compounds. J. Phys. Chem. 1969, 73, 1774–1780.
22. Bragg, W.L.; Gottfried, C.; West, J. The Structure of β Alumina. Z. Krist. Cryst. Mater. 1931, 77, 255–274.
23. Wolfenstine, J.; Allen, J.; Sumner, J.; Sakamoto, J. Electrical and mechanical properties of hot-pressed versus sintered LiTi2(PO4)3. Solid State Ionics 2009, 180, 961–967.
24. Wang, B.; Chakoumakos, B.C.; Sales, B.; Kwak, B.; Bates, J. Synthesis, Crystal Structure, and Ionic Conductivity of a Polycrystalline Lithium Phosphorus Oxynitride with the γ-Li3PO4 Structure. J. Solid State Chem. 1995, 115, 313–323.
25. Bates, J.B.; Dudney, N.J.; Neudecker, B.; Ueda, A.; Evans, C.D. Thin-film lithium and lithium-ion batteries. Solid State Ionics 2000, 135, 33–45.

26. Catti, M. Local structure of the Li1/8La5/8TiO3(LLTO) ionic conductor by theoretical simulations. J. Phys. Conf. Ser. 2008, 117, 12008.
27. Harada, Y.; Ishigaki, T.; Kawai, H.; Kuwano, J. Lithium ion conductivity of polycrystalline perovskite La0.67âˆ’xLi3xTiO3 with ordered and disordered arrangements of the A-site ions. Solid State Ionics 1998, 108, 407–413.
28. Thangadurai, V.; Kaack, H.; Weppner, W.J.F. Novel Fast Lithium Ion Conduction in Garnet-Type Li5La3M2O12(M = Nb, Ta). J. Am. Ceram. Soc. 2003, 86, 437–440.
29. Murugan, R.; Thangadurai, V.; Weppner, W. Fast Lithium Ion Conduction in Garnet-Type Li7La3Zr2O12. Angew. Chem. Int. Ed. 2007, 46, 7778–7781.
30. Ramakumar, S.; Janani, N.; Murugan, R. Influence of lithium concentration on the structure and Li+ transport properties of cubic phase lithium garnets. Dalton Trans. 2014, 44, 539–552.
31. Awaka, J.; Kijima, N.; Hayakawa, H.; Akimoto, J. Synthesis and structure analysis of tetragonal Li7La3Zr2O12 with the garnet-related type structure. J. Solid State Chem. 2009, 182, 2046–2052.
32. Awaka, J.; Takashima, A.; Kataoka, K.; Kijima, N.; Idemoto, Y.; Akimoto, J. Crystal Structure of Fast Lithium-ion-conducting Cubic Li7La3Zr2O12. Chem. Lett. 2011, 40, 60–62.
33. Bernstein, N.; Johannes, M.D.; Hoang, K. Origin of the Structural Phase Transition inLi7La3Zr2O12. Phys. Rev. Lett. 2012, 109, 205702.
34. Meier, K.; Laino, T.; Curioni, A. Solid-State Electrolytes: Revealing the Mechanisms of Li-Ion Conduction in Tetragonal and Cubic LLZO by First-Principles Calculations. J. Phys. Chem. C 2014, 118, 6668–6679.
35. Kühne, T.D.; Iannuzzi, M.; Del Ben, M.; Rybkin, V.V.; Seewald, P.; Stein, F.; Laino, T.; Khaliullin, R.Z.; Schütt, O.; Schiffmann, F.; et al. CP2K: An electronic structure and molecular dynamics software package—Quickstep: Efficient and accurate electronic structure calculations. J. Chem. Phys. 2020, 152, 194103.
36. Liu, K.; Ma, J.-T.; Wang, C.-A. Excess lithium salt functions more than compensating for lithium loss when synthesizing Li6.5La3Ta0.5Zr1.5O12 in alumina crucible. J. Power Sources 2014, 260, 109–114.
37. Rangasamy, E.; Wolfenstine, J.; Sakamoto, J. The role of Al and Li concentration on the formation of cubic garnet solid electrolyte of nominal composition Li7La3Zr2O12. Solid State Ionics 2012, 206, 28–32.
38. Yoo, A.R.; A Yoon, S.; Kim, Y.S.; Sakamoto, J.; Lee, H.C. A Comparative Study on the Synthesis of Al-Doped Li6.2La3Zr2O12 Powder as a Solid Electrolyte Using Sol–Gel Synthesis and Solid-State Processing. J. Nanosci. Nanotechnol. 2016, 16, 11662–11668.

39. Gao, Y.; Wang, X.; Wang, W.; Zhuang, Z.; Zhang, D.; Fang, Q. Synthesis, ionic conductivity, and chemical compatibility of garnet-like lithium ionic conductor Li5La3Bi2O12. Solid State Ionics 2010, 181, 1415–1419.
40. Jin, Y.; McGinn, P.J. Al-doped Li7La3Zr2O12 synthesized by a polymerized complex method. J. Power Sources 2011, 196, 8683–8687.
41. Park, J.S.; Cheng, L.; Zorba, V.; Mehta, A.; Cabana, J.; Chen, G.; Doeff, M.M.; Richardson, T.J.; Park, J.H.; Son, J.-W.; et al. Effects of crystallinity and impurities on the electrical conductivity of Li–La–Zr–O thin films. Thin Solid Films 2015, 576, 55–60.
42. Tan, J.; Tiwari, A. Fabrication and Characterization of Li7La3Zr2O12 Thin Films for Lithium Ion Battery. ECS Solid State Lett. 2012, 1, Q57–Q60.
43. Zhang, Y.; Chen, F.; Tu, R.; Shen, Q.; Zhang, L. Field assisted sintering of dense Al-substituted cubic phase Li7La3Zr2O12 solid electrolytes. J. Power Sources 2014, 268, 960–964.
44. Kobayashi, Y.; Miyashiro, H.; Takeuchi, T.; Shigemura, H.; Balakrishnan, N.; Tabuchi, M.; Kageyama, H.; Iwahori, T. All-solid-state lithium secondary battery with ceramic/polymer composite electrolyte. Solid State Ionics 2002, 152–153, 137–142.